Intramolecular vibronic dynamics in molecular solids

Kjeldgaard, L.; Kaambre, T.; Schiessling, J.; Marenne, I.; O'Shea, J.N.; Schnadt, J.; Glover, C.J.; Nagasono, M.; Nordlund, D.; Garnier, M.G.

Published in:
Physical Review B

DOI:
10.1103/physrevb.72.205414

Publication date:
2005

Intramolecular vibronic dynamics in molecular solids: C_{60}

L. Kjeldgaard,[1,*] T. Käämbre,[1,†] J. Schiessling,[1,‡] I. Marenne,[2] J. N. O'Shea,[1,§] J. Schnadt,[1,‖] C. J. Glover,[3,¶] M. Nagasono,[3,**] D. Nordlund,[3] M. G. Garnier,[3,††] L. Qian,[1] J.-E. Rubensson,[1] P. Rudolf,[4,2] N. Mårtensson,[1,3] J. Nordgren,[1] and P. A. Brühwiler[1,5,‡‡]

[1]*Department of Physics, Uppsala University, Box 530, SE-751 21 Uppsala, Sweden*

[2]*LISE, Facultès Universitaires Notre Dame de la Paix, Rue de Bruxelles 61, B-5000 Namur, Belgium*

[3]*MAX-lab, University of Lund, Box 118, SE-221 00 Lund, Sweden*

[4]*Materials Science Centre, University of Groningen, Nijenborgh 4, NL-9747 AG Groningen, The Netherlands*

[5]*Empa, Materials Science and Technology, Lerchenfeldstrasse 5, CH-9014 St. Gallen, Switzerland*

(Received 9 June 2005; published 9 November 2005)

Vibronic coupling in solid C_{60} has been investigated with a combination of resonant photoemission spectroscopy (RPES) and resonant inelastic x-ray scattering (RIXS). Excitation as a function of energy within the lowest unoccupied molecular orbital resonance yielded strong oscillations in intensity and dispersion in RPES, and a strong inelastic component in RIXS. Reconciling these two observations establishes that vibronic coupling in this core hole excitation leads to predominantly inelastic scattering and localization of the excited vibrations on the molecule on a femtosecond time scale. The coupling extends throughout the widths of the frontier valence bands.

DOI: 10.1103/PhysRevB.72.205414 PACS number(s): 79.60.Jv, 33.60.−q, 68.43.Fg, 73.22.−f

Molecular solids based on aromatic molecules and their derivatives are being studied widely and exploited for their great potential in electronic devices.[1–4] Thanks to their relatively simple electronic structure, C_{60} compounds have been studied heavily and can be considered as prototypes for these aromatic solids. One aspect of interest is the vibronic coupling in these systems, since this is relevant for a range of interesting processes, including femtochemistry,[5] molecular dissociation,[6] and superconductivity.[7]

For isolated molecules, such coupling can be explained theoretically in great detail,[8] and resolved experimentally down to a femtosecond time scale.[9] For molecular solids, however, such dynamics become more difficult to access. Studies on isolated C_{60} molecules have established that there is stronger vibronic coupling to a hole in the highest occupied molecular orbital (HOMO) than to an electron in the lowest unoccupied molecular orbital (LUMO).[8,10–12] In C_{60} multilayers, solid-state band structure in the HOMO has not been observed, leading to contrasting viewpoints in the interpretation of experimental results on the strength of vibrational coupling.[11,13–19] Some workers have claimed that vibrational coupling is much smaller in the solid than for the isolated molecule.[17,18] Theoretical work, which did not consider vibrations,[14] shows that orientational disorder and the relatively large unit cell could explain some aspects of the experimental observations.[13,15–18] Experimental data at the critical points[16] differ strongly from the calculated results, however, suggesting that theory is far from a complete understanding. More recent experimental work has shown a significant role of such vibrational coupling for the HOMO in two dimensions[11] and for exciton dynamics in three dimensions.[19] These observations are difficult to reconcile with previous claims, suggesting that a new approach yielding more direct information on the vibrational coupling in such solids is needed.

Resonant photoemission spectroscopy (RPES) and resonant inelastic soft-x-ray scattering (RIXS) are core level excitation-deexcitation techniques which give access to electron dynamics on the femtosecond time scale.[20] Here, we apply these techniques in concert, to probe the dynamics of vibronic interactions.

Our experiments were carried out at Beamline I511 (Ref. 21) at MAX-lab in Lund, Sweden. The rotatable endstation is equipped with a Scienta SES-200 hemispherical electron analyzer[22] and an XES-300 soft x-ray emission spectrometer.[23] C_{60} multilayers were deposited *in situ* onto the clean (111) surface of a Cu crystal. Photoelectron spectra (PES) were acquired at an overall resolution of 150 meV. The photon energy resolution of RPES and RIXS was 100 meV, and these spectra were collected with an energy resolution of 56 meV for the electrons and 150 meV for the x rays, respectively. PES and RPES were taken in near-normal emission, with a deviation of 8° in one direction from normal due to the construction of the measurement chamber.[24]

We illustrate the electronic transitions of the applied experimental techniques in Fig. 1(a). In x-ray absorption spectroscopy (XAS) a 1*s* electron is promoted into a previously unoccupied electronic state. RPES and RIXS are described in a two-step picture. The first step is common for both techniques, consisting of the absorption of a photon, identical to XAS. In the second step different decay channels are examined. The excited state decays with the emission of (1) a valence electron in RPES or (2) an x-ray photon in RIXS.

In the first step of both resonant processes, RPES and RIXS, absorption into a specific distribution of vibrational states is involved,[20,25] determined by the photon energy and bandwidth via the appropriate Franck-Condon factors. Moderate control of the vibrational excitations of each electronic state is exerted by tuning the photon energy.[6,20] To illustrate the vibrational aspects, we show a simplified Franck-Condon diagram in Fig. 1(b). In the PES final state the ground-state vibrational wave function is projected onto the manifold of the $5h_u^{-1}$ hole state.[8,26] A similar projection is reflected in XAS. The two resonant processes differ as follows: (1)

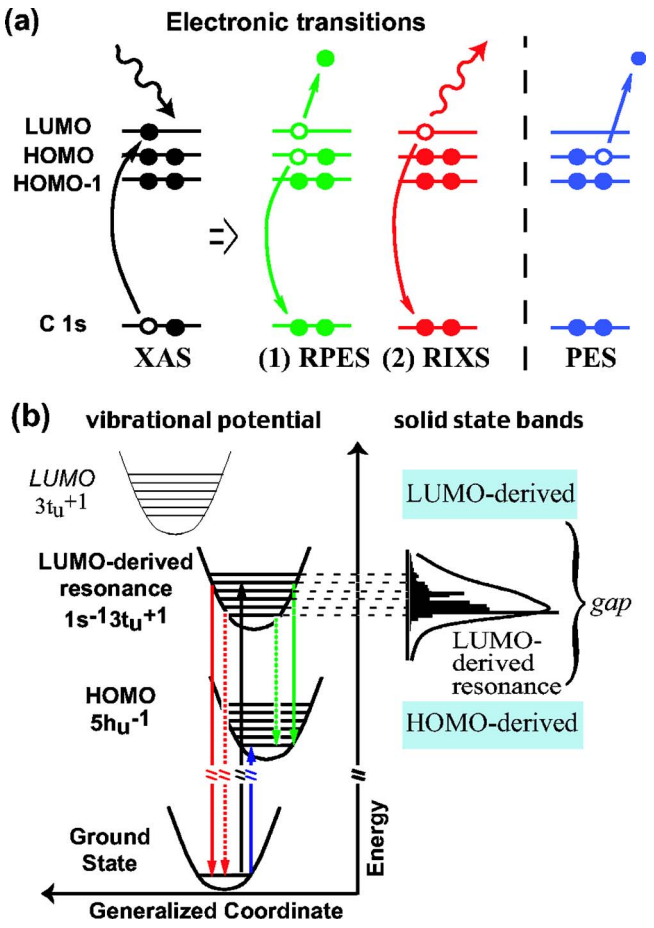

FIG. 1. (Color online) (a) A schematic of the spectroscopies employed, showing the relationships between the intermediate and final electronic states. Photoemission (PES) and resonant photoemission (RPES) have the same final state, whereas resonant inelastic soft-x-ray emission (RIXS) leaves the molecule in its ground state. (b) (left) A simplified Franck-Condon diagram shows vibrational potentials for the ground, valence-hole $5h_u^{-1}$, and $1s$ excited $1s^{-1}3t_u^{+1}$ states. The transitions depicted in (a) are indicated by solid arrows in the corresponding colors; dashed arrows suggest the role of energy dissipation in the intermediate state. (b) (right) The LUMO-derived resonance is located in the fundamental gap formed by the solid-state HOMO- and LUMO-derived-bands (Ref. 20). The simulation in terms of vibrational excitation, cf. Fig. 2, suggests a plausible distribution of the observed spectral linewidth.

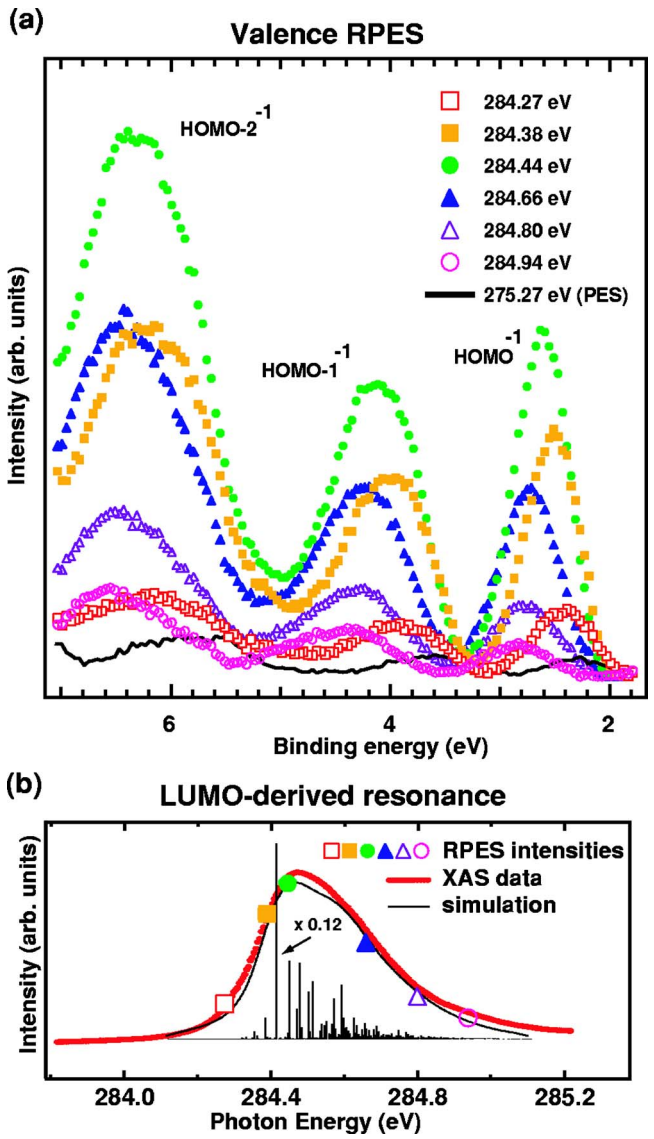

FIG. 2. (Color online) (a) RPES and direct PES data for solid C_{60}, taken at the indicated photon energies. For each RPES spectrum the direct PES contribution shown has been subtracted from raw RPES data. The molecular levels are labeled; uppercase indices indicate the valence-hole final state. (b) Simulation and XAS data taken at the LUMO-derived resonance. The (0,0) line of the simulation is rescaled by 0.12 for better comparison. The variation of the RPES signal is plotted by symbols on the curve. The value of each symbol corresponds to the peak areas of the respective valence band spectrum shown in (a). See the text for more details.

RPES projects the excited state onto the same manifold as PES; (2) RIXS projects it back onto the ground-state vibrational manifold. By varying the excitation energy through the LUMO-derived resonance, one increases the degree of intermediate vibrational excitation. Thus, by comparing both final states complementary information is accessible, allowing one to measure the effects of vibronic coupling as we will discuss below.

The RPES spectra are displayed in Fig. 2(a). We note that the main feature in these spectra disperses almost linearly with increasing excitation energy. The magnitude of the shift can be appreciated by comparison of, e.g., the curves collected for $h\nu$=284.27 eV and for $h\nu$=284.94 eV. The peaks shift up to half the energy separation between the peaks of the direct PES data, which is a dramatic effect on the scale of observed electronic energy dispersion.[17,18] We assign this RPES energy dispersion solely to vibrational interactions, because, as illustrated in Fig. 1(b), the LUMO-derived resonance in the core excited state is lowered in energy, forming an exciton in the fundamental band gap[12,20,27,28] of C_{60}, and hence cannot exchange energy with other electronic states in a first-order process.

As already suggested in the discussion of Fig. 1, vibrational structure determines the line shapes of the LUMO-derived resonance. A simulation of its vibrational structure is

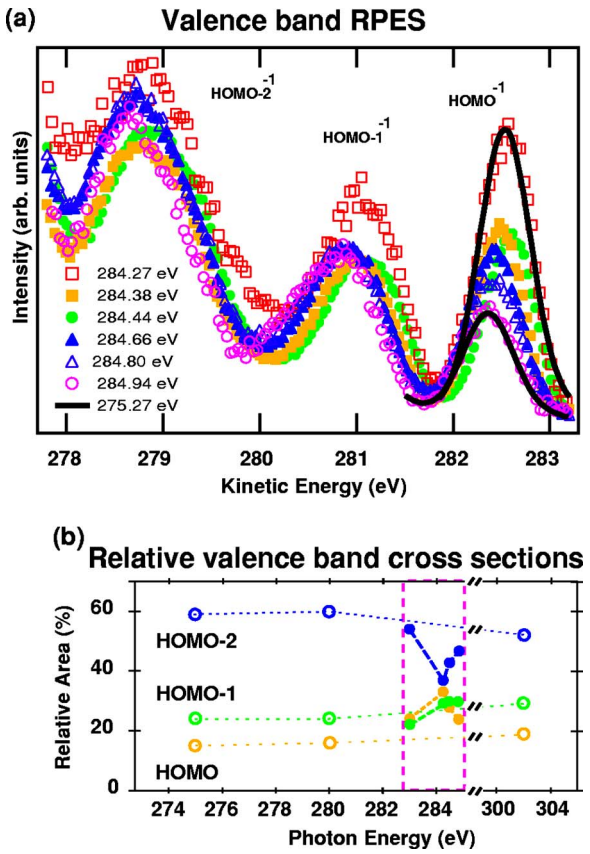

FIG. 3. (Color online) (a) The spectra from Fig. 2 normalized to the area of the HOMO-2 structure as explained in the text, plotted on a kinetic energy scale. Two line shapes of the HOMO from direct photoemission, rescaled to match the extremal intensities of RPES and separated by 0.19 eV, are shown for comparison of line shape and energy separation for the two extreme cases in RPES. (b) Evolution of the peak areas of the three valence structures while exciting across the LUMO-derived resonance. Direct PES (RPES) is shown as open (filled) circles. Within the interval 284 to 285 eV, the contribution from direct photoemission has been subtracted from the raw RPES signal.

presented in Fig. 2(b). The model (vertical lines) shown embodies linear coupling at finite temperature.[11,29] A convolution of the model (narrow solid line) with a 0.1 eV wide Lorentzian to account for the core hole lifetime and a 0.06 eV wide Gaussian for the energy resolution compares well with the overall shape of the experimental spectrum. The goal of the simulation is not a unique distribution of vibronic states, which would be well beyond the scope of this work, but is a guide to the number and density of states available. To examine the role of the core vibronic coupling, we display the variation in RPES cross section in Fig. 2(b). We first note that the total intensity variations in the RPES largely follow that of the LUMO-derived resonance for all three bands, as previously shown in less detail.[30] This can be taken as confirmation that the excitation of the C 1*s* electron is the dominant process in our data, ruling out significant contributions from interference between PES and RPES as a possible explanation for the observed gross intensity variations.[20]

In Fig. 3(a) we show that the RPES data are almost constant in kinetic energy despite the large increase in photon energy. This is in contradiction to the common observation of linear dispersion for participant decay.[20] To investigate intensity variations within the RPES data, the spectra shown in Fig. 3(a) have been normalized to the area of the HOMO-2 structure.[31] While in direct PES the relative intensities are almost constant at these photon energies, the resonant spectra show strong variations within each band.

The variation in the relative peak intensities is displayed in Fig. 3(b). Above, we already discussed one reason why we rule out possible effects of interference between RPES and PES for the absolute cross sections. Further support is given by measurements taken at two orientations of light polarization and electron emission. In one geometry the light polarization was parallel, in the other perpendicular, to the electron emission direction.[32] The results were identical, showing that interference between PES and RPES is not responsible for the observed variations.[20,33] Thus, the variation in relative cross section shown in Fig. 3 must be due to the particular vibrational configuration produced in the excitation step.

Generally, within the Born-Oppenheimer approximation, electronic transition cross sections are expected to be a purely electronic property (see, e.g., Ref. 34). Therefore, the RPES peaks are expected to exhibit constant relative intensity as one changes the number and type of vibrations excited, in contrast to the present observation. Many of the *intra*molecular vibrational modes of C_{60} are nontotally symmetric, however, and should couple to the excitation into the LUMO-derived resonance, thereby mixing different electronic configurations in XAS;[25] we attribute the present observations to this coupling. This phenomenon has already been shown to lead to parity mixing in the radiative transitions,[6,35–37] but we assume that all Jahn-Teller modes could also contribute. To our knowledge, only small molecules show comparable variations in the RPES cross section.[38,39]

Since the cross section of each peak in the frontier valence spectrum (HOMO, HOMO-1, HOMO-2) varies almost uniformly in RPES, all the molecular level-derived bands contain the vibrational character implicit in the coupling described above over their entire width.

Crucial details of the vibronic coupling emerge in the RIXS spectra. In Fig. 4 two peaks can be resolved in the spectra; one distinct feature follows the excitation energy (which is the so-called elastic peak, clearly visible for the spectra taken at $h\nu \geqslant 284.65$ eV as a shoulder or major peak) and a peak at a constant emission energy of $\approx$284.4 eV, with weak structures surrounding these two. The elastic peak is due primarily to diffuse reflection of the incoming photon beam, and the intensity should in general be highly dependent on, e.g., surface roughness. Therefore, we postulate a certain contribution from this source in all spectra. The rest of the spectrum is the RIXS participant signal. The data in Fig. 4 show that the strongest contribution to the latter is emitted at an almost constant energy, just as we observe in RPES.[40]

Since RPES and RIXS probe different final states, there are two scenarios which can explain our observations. (1) Looking at Fig. 1(b), one possibility would be that the effective vibronic potentials of the ground state, PES final state,

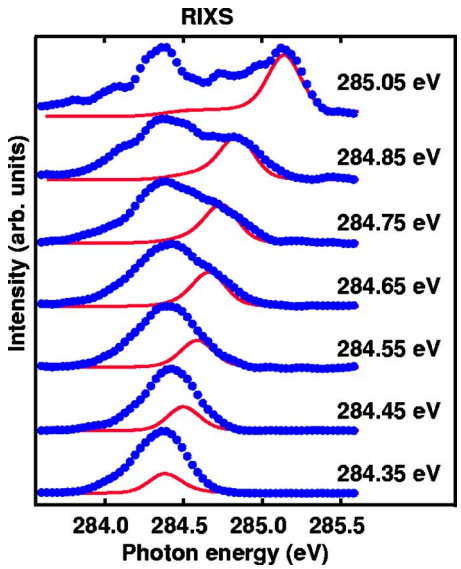

FIG. 4. (Color online) RIXS data (dotted lines) taken at photon energies similar to the RPES data. The position of the elastic peak is indicated by a Gaussian (solid lines) centered at the incident photon energy. In the lowest three spectra the intensity of the elastic peak is estimated by the constraint that the result of subtracting the elastic peak should not induce structures not already apparent in the raw data.

and XAS final state (LUMO-derived resonance) are all parallel, so that transitions among the vibrational levels during deexcitation should be suppressed.[41] However, this is ruled out directly based on the observed strong coupling in PES (Refs. 8 and 11) and XAS (simulation in Fig. 2), showing that the ground-state potential is strongly shifted from both excited-state potentials. (2) The remaining possible explanation is that the strongest transition always proceeds from (almost) the same vibrational component in the intermediate state, although we explicitly vary the vibrational component of this state in the excitation step by tuning the photon energy. This would require a dissipation of vibrational energy in the intermediate state, placing the system effectively at the (0,0) transition. The deexcitation step for this scenario is suggested by dashed lines in Fig. 1(b). Since the deexcitation proceeds on a 5 fs time scale,[20,27] this requires a rapid decoupling of the vibrations from the excited electronic state.

In the solid state such rapid decoupling was long ago incorporated in phenomenological models in which the excited vibrations can dissipate into the rest of the solid.[42,43] This is found often to quench a coherent coupling upon deexcitation, which would explain the overall energy loss as observed here. In molecular solids, however, the intermediate electronic state is localized on a single molecule.[20] In these systems, only intramolecular vibrations couple strongly in XAS, which has been shown, e.g., by the minimal effects of changing the local environment from C_{60} solid to Xe matrix[27] to gas phase.[44] The observation of very weak coupling to neighboring molecules is reasonable, considering the relatively large spacing between molecules in the solid (~3.0 Å shell-to-shell), compared to the covalent bond length (~1.4 Å). We also note that *inter*molecular vibrations are characterized by a time scale significantly larger than the core hole lifetime of 5.6 fs, whereas *intra*molecular vibrations oscillate on a comparable time scale.[45] Thus, the vibrations created in XAS must be considered localized on the probe molecule, but decoupled from the deexcitation process. Simulations of an atomic collision with C_{60} show that the time for a vibrational pulse to travel from the front to the back of the molecule is much larger,[46] supporting the inference that an intramolecular vibrational pulse produced in the excitation step could disperse away from the core-excited atom, while remaining on the probed molecule.

The conclusion that the vibrations remain on the molecule provides a natural explanation of the cross-section observations in Fig. 3—the vibrations continue to interact with the (spatially distributed) electronic states, thereby affecting their symmetry, and thus their overlap with the core hole. These effects should be level dependent, as observed. The present observations offer an explanation of similar shifts measured in RPES for polymers[47] and biisonicotinic acid multilayers.[48]

To conclude, we combine resonant inelastic x-ray scattering and photoemission spectroscopies to study solid C_{60}. We find evidence that the vibrations produced in the excitation step remain to a measurable degree on the probed molecule, affecting the given deexcitation step within an effective time scale of 5 fs. The present study shows that vibronic character extends throughout the observed electronic bands, in contrast to earlier claims.[17,18] We also show that strong coupling between electronic and vibrational excitation on a single molecule leads to dephasing effects on the few-femtosecond time scale.

Since the behavior observed here corresponds to that of macroscopic systems, the C_{60} molecule can be said to lie in the macroscopic domain of core hole vibronic coupling. Smaller aromatic molecules should provide further intermediate cases for study of this problem.

We would like to acknowledge H. Köppel, L. S. Cederbaum, N. Manini, P. Hedegaard, and E. Tosatti for stimulating and useful discussions. This work was supported by the European Union (TMR Contract ERB FMRX-CT 970155), FOM (Netherlands), and the Consortium on Clusters and Ultrafine Particles, which is funded by Stiftelsen för Strategisk Forskning. L. K. thanks the National Natural Science Research Council (SNF).

*Present address: MAX-lab, University of Lund, Box 118, SE-221 00 Lund, Sweden.

†Present address: Institute of Physics, Tartu University, Riia 142, EE-51014 Tartu, Estonia.

‡Corresponding author. Email address: joachim.schiessling@fysik.uu.se; Present address: MAX-lab, University of Lund, Box 118, SE-221 00 Lund, Sweden.

§Present address: School of Physics and Astronomy, University of

Nottingham, Nottingham, NG7 2RD, United Kingdom.
[‖]Present address: Department of Physics and Astronomy, University of Aarhus, Ny Munkegade, 8000 Aarhus C, Denmark.
[¶]Present address: Department of Electronic Materials Engineering, Research School of Physical Sciences and Engineering, Australian National University Canberra, Australia.
**Present address: Universität Hamburg, Luruper Chausee 149, 22761 Hamburg, Germany.
[††]Present address: Institut de Physique, Université de Neuchâtel rue Breguet 1, 2000 Neuchâtel, Switzerland.
[‡‡]Corresponding author. Email address: paul.bruehwiler@empa.ch

[1] C. Joachim, J. K. Gimzewski, and A. Aviram, Nature **408**, 541 (2000).
[2] H. Park, J. Park, A. K. L. Lim, E. H. Anderson, A. P. Alivisatos, and P. L. McEuen, Nature **407**, 57 (2000).
[3] P. K. H. Ho, J.-S. Kim, J. H. Burroughes, H. Becker, S. F. Y. Li, T. M. Brown, F. Cacialli, and R. H. Friend, Nature **404**, 481 (2000).
[4] J. A. Theobald, N. S. Oxtoby, M. A. Philips, N. R. Champness, and P. H. Beton, Nature **424**, 1029 (2003).
[5] R. J. D. Miller, G. L. McLendon, A. J. Nozik, W. Schmickler, and F. Willig, *Surface Electron Transfer Processes* (VCH, New York, 1995).
[6] F. K. Gel'mukhanov and H. Ågren, Phys. Rep. **312**, 87 (1999).
[7] O. Gunnarsson, Rev. Mod. Phys. **69**, 575 (1997).
[8] N. Manini, P. Gattari, and E. Tosatti, Phys. Rev. Lett. **91**, 196402 (2003).
[9] M. Z. Zgierski, T. Seideman, and A. Stolow, Nature **401**, 52 (1999).
[10] O. Gunnarsson, H. Handschuh, P. S. Bechthold, B. Kessler, G. Ganteför, and W. Eberhardt, Phys. Rev. Lett. **74**, 1875 (1995).
[11] P. A. Brühwiler, A. J. Maxwell, P. Baltzer, S. Andersson, D. Arvanitis, L. Karlsson, and N. Mårtensson, Chem. Phys. Lett. **279**, 85 (1997).
[12] P. Rudolf, M. S. Golden, and P. A. Brühwiler, J. Electron Spectrosc. Relat. Phenom. **100**, 409 (1999).
[13] J. Wu, Z.-X. Shen, D. S. Dessau, R. Cao, D. S. Marshall, P. Pianetta, I. Lindau, X. Yang, J. Terry, D. M. Kings, B. O. Wells, D. Elloway, H. R. Wendt, C. A. Brown, H. Hunziker, and M. S. de Vries, Physica C **197**, 251 (1992).
[14] E. L. Shirley and S. G. Louie, Phys. Rev. Lett. **71**, 133 (1993).
[15] G. Gensterblum, J.-J. Pireaux, P. A. Thiry, R. Caudano, T. Buslaps, R. L. Johnson, G. LeLay, V. Aristov, R. Günther, A. Taleb-Ibrahimi, G. Indlekofer, and Y. Petroff, Phys. Rev. B **48**, R14756 (1993).
[16] M. Merkel, M. Knupfer, M. S. Golden, J. Fink, R. Seemann, and R. L. Johnson, Phys. Rev. B **47**, 11470 (1993).
[17] P. J. Benning, C. G. Olson, D. W. Lynch, and J. H. Weaver, Phys. Rev. B **50**, R11239 (1994).
[18] G. Gensterblum, J. Electron Spectrosc. Relat. Phenom. **81**, 89 (1996).
[19] J. P. Long, S. J. Chase, and M. N. Kabler, Phys. Rev. B **64**, 205415 (2001).
[20] P. A. Brühwiler, O. Karis, and N. Mårtensson, Rev. Mod. Phys. **74**, 703 (2002).
[21] R. Denecke, P. Väterlein, M. Bässler, N. Wassdahl, S. M. Butorin, A. Nilsson, J.-E. Rubensson, J. Nordgren, N. Mårtensson, and R. Nyholm, J. Electron Spectrosc. Relat. Phenom. **103**, 971 (1999).
[22] N. Mårtensson, P. Baltzer, P. A. Brühwiler, J.-O. Forsell, A. Nilsson, A. Stenbor, and B. Wannberg, J. Electron Spectrosc. Relat. Phenom. **70**, 117 (1994).
[23] J. Nordgren, G. Bray, S. Cramm, R. Nyholm, J.-E. Rubensson, and N. Wassdahl, Rev. Sci. Instrum. **60**, 1690 (1989).
[24] J. Schiessling, L. Kjeldgaard, T. Käämbre, I. Marenne, J. N. O'Shea, J. Schnadt, C. J. Glover, M. Nagasono, D. Nordlund, M. G. Garnier, L. Qian, J.-E. Rubensson, P. Rudolf, N. Mårtensson, J. Nordgren, and P. A. Brühwiler, Phys. Rev. B **71**, 165420 (2005).
[25] H. Köppel, F. X. Gadea, G. Klatt, J. Schirmer, and L. S. Cederbaum, J. Chem. Phys. **106**, 4415 (1997).
[26] S. Hüfner, *Photoelectron Spectroscopy* (Springer-Verlag, Berlin, 1996).
[27] P. A. Brühwiler, A. J. Maxwell, P. Rudolf, C. D. Gutleben, B. Wästberg, and N. Mårtensson, Phys. Rev. Lett. **71**, 3721 (1993).
[28] J. Schnadt, J. Schiessling, and P. A. Brühwiler, Chem. Phys. **312**, 39 (2005).
[29] V. P. Antropov, O. Gunnarsson, and A. I. Liechtenstein, Phys. Rev. B **48**, 7651 (1993).
[30] P. A. Brühwiler, A. J. Maxwell, A. Nilsson, R. L. Whetten, and N. Mårtensson, Chem. Phys. Lett. **193**, 313 (1992).
[31] The HOMO-2 peaks do not all show the same height due to differences in the Auger background (not shown).
[32] In order to minimize the PES contribution in the spectra, all data shown are taken in the perpendicular geometry.
[33] M. Weinelt, A. Nilsson, M. Magnuson, T. Wiell, N. Wassdahl, O. Karis, A. Föhlisch, N. Mårtensson, J. Stohr, and M. Samant, Phys. Rev. Lett. **78**, 967 (1997).
[34] J. M. Ziman, *Principles of the Theory of Solids*, 2nd ed. (Cambridge University Press, Cambridge, 1984).
[35] P. Skytt, P. Glans, J.-H. Guo, K. Gunnelin, C. Såthe, J. Nordgren, F. K. Gel'mukhanov, A. Cesar, and H. Ågren, Phys. Rev. Lett. **77**, 5035 (1996).
[36] J.-H. Guo, P. Glans, P. Skytt, N. Wassdahl, J. Nordgren, Y. Luo, H. Ågren, Y. Ma, T. Warwick, P. Heimann, E. Rotenberg, and J. D. Denlinger, Phys. Rev. B **52**, 10681 (1995).
[37] Y. Luo, H. Ågren, F. Gel'mukhanov, J. Guo, P. Skytt, N. Wassdahl, and J. Nordgren, Phys. Rev. B **52**, 14479 (1995).
[38] M. N. Piancastelli, M. Neeb, A. Kivimäki, B. Kempgens, H. M. Köppe, K. Maier, and A. M. Bradshaw, Phys. Rev. Lett. **77**, 4302 (1996).
[39] V. Carravetta, F. K. Gel'mukhanov, H. Ågren, S. Sundin, S. J. Osborne, A. Naves de Brito, O. Bjoorneholm, A. Ausmees, and S. Svensson, Phys. Rev. A **56**, 4665 (1997).
[40] We note that the intensity of the RIXS signal follows that of the XAS cross section. We take this as support for the approximate separation between RIXS signal and elastic peak of the RIXS data in Fig. 4.
[41] O. Björneholm, A. Nilsson, A. Sandell, B. Hernnäs, and N. Mårtensson, Phys. Rev. B **49**, 2001 (1994).
[42] G. D. Mahan, Phys. Rev. B **15**, 4587 (1977).
[43] C.-O. Almbladh, Phys. Rev. B **16**, 4343 (1977).
[44] S. Krummacher, M. Biermann, M. Neeb, A. Liebsch, and W. Eberhardt, Phys. Rev. B **48**, 8424 (1993).
[45] A. M. Rao, P. C. Eklund, J.-L. Hodeau, L. Marques, and M. Nunez-Regueiro, Phys. Rev. B **55**, 4766 (1997).
[46] V. Bernshtein and I. Oref, Chem. Phys. Lett. **313**, 52 (1999).
[47] R. Friedlein, S. L. Sorensen, A. Baev, F. Gel'mukhanov, J. Birgerson, A. Crispin, M. P. de Jong, W. Osikowicz, C. Murphy, H. Ågren, and W. R. Salaneck, Phys. Rev. B **69**, 125204 (2004).
[48] J. Schnadt, L. Patthey, J. N. O'Shea, and P. A. Brühwiler (unpublished).